# Electronic Supplementary Material

## Ultrathin microcrystalline hydrogenated Si/Ge alloyed tandem solar cells towards full solar spectrum conversion

**Yu Cao[1,2], Xinyun Zhu[1,2], Xingyu Tong[1,2], Jing Zhou(✉)[3], Jian Ni[4], Jianjun Zhang[4], Jinbo Pang(✉)[5]**

1 Key Laboratory of Modern Power System Simulation and Control & Renewable Energy Technology, Ministry of Education (Northeast Electric Power University), Jilin 132012, China

2 School of Electrical Engineering, Northeast Electric Power University, Jilin 132012, China

3 School of Chemical Engineering, Northeast Electric Power University, Jilin 132012, China

4 Key Laboratory of Photo-electronics Thin Film Devices and Technique of Tianjin, Institute of Photo-electronic Thin Film Devices and Technology, College of Electronic Information and Optical Engineering, Nankai University, Tianjin 300350, China

5 Collaborative Innovation Center of Technology and Equipment for Biological Diagnosis and Therapy in Universities of Shandong, Institute for Advanced Interdisciplinary Research (iAIR), University of Jinan, Jinan 250022, China

E-mails: zhoujing@neepu.edu.cn (Zhou J); jinbo.pang@hotmail.com, ifc_pangjb@ujn.edu.cn (Pang J)

## S.1 Material input parameters

The simulator adopted in this work is wxAMPS, which is an updated version of the AMPS (Analysis of Microelectronic and Photonic Structure) [1, 2]. This simulator can not only calculate the basic parameters of solar cells, but also output the EQE response of each sub-cell in the multi-junction TFSC, which is a useful tool for simulating and analyzing the photovoltaic characteristics of multi-junction TFSCs

[3-9].

In the quadruple junction TFSC model, the n-a-Si:H (15 nm)/p-μc-Si:H (5 nm)/p-a-SiC:H (15 nm) was used as the top/second tunnel recombination junction. The n-a-Si:H (15 nm)/p-μc-Si:H (20 nm) was used as the second/third and third/bottom tunnel recombination junctions. It should be noted that we did not introduce buffer layer in a/μc-SiGe:H sub-cells with high Ge content to further optimize the device performance. Since the wx-AMPS cannot simulate the trapping effect of the front electrode, which, however, plays a crucial role in the TFSCs. Therefore, the absorption coefficient of the silicon based thin films was modified. Firstly, the thickness of the silicon based intrinsic layer in the device model was set as the same as that in the literature. Then, the absorption coefficient was carefully adjusted to make the simulated EQE curves match the experimental results in the literature as much as possible. By this way our simulation results can be closer to the actual device. The reflection coefficients of the front and back electrodes were set to be 0 and 1, respectively. The Air Mass 1.5 solar radiation spectrum was employed as the illuminating source. The thickness of the amorphous silicon-based sub-cells varied from 0 to1 μm, and that of the microcrystalline silicon-based sub-cells varied from 0 to 8 μm. The absorption coefficients of all the intrinsic layers were derived from our experimental results and reported studies [10]. It was assumed that the band-gap of the a-$Si_{1-x}Ge_x$:H intrinsic layers varied linearly from 1.78 to1.1 eV along with the increase of x from 0 to 100%, and that of the μc-$Si_{1-y}Ge_y$:H intrinsic layers varied linearly from 1.1 to 0.66 eV along with the increase of y from 0 to 100% [11].The

defect density of the a/μc-SiGe:H intrinsic layers increased from $10^{14}$ to $10^{16}$ $cm^{-3}$ with increasing Ge content from 0 to 100% [11]. The input parameters of each layer are summarized in Table S1.

Table S1. Material input parameters

| Parameters | p-a-SiC:H | i-a-Si:H | i-a-SiGe:H | n-a-Si:H | p-μc-Si:H | i-μc-Si:H | i-μc-SiGe:H |
|---|---|---|---|---|---|---|---|
| Band-gap/eV | 2 | 1.78 | 1.78-1.1 | 1.78 | 1.18 | 1.1 | 1.1-0.66 |
| Electron affinity/eV | 3.89 | 4 | 4 | 4 | 4 | 4 | 4 |
| Electron mobility/($cm^2$/V/s) | 20 | 20 | 20 | 20 | 32 | 32 | 32 |
| Hole mobility/($cm^2$/V/s) | 4 | 4 | 4 | 4 | 8 | 8 | 8 |
| Effective DOS in bands/$cm^{-3}$ | $2\times10^{20}$ | $2\times10^{20}$ | $2\times10^{20}$ | $2\times10^{20}$ | $2\times10^{20}$ | $2\times10^{20}$ | $2\times10^{20}$ |
| Donor doping density/$cm^{-3}$ | 0 | 0 | 0 | $1.6\times10^{19}$ | 0 | 0 | 0 |
| Accepter doping density/$cm^{-3}$ | $1.6\times10^{19}$ | 0 | 0 | 0 | $1.6\times10^{19}$ | 0 | 0 |
| Gaussian Defects Density/$cm^{-3}$ | $4\times10^{17}$ | $10^{14}$ | $10^{14}$-$10^{16}$ | $8\times10^{16}$ | $4\times10^{17}$ | $10^{14}$ | $10^{14}$-$10^{16}$ |

## S.2 Comparison with experimental results

Fig. S1 shows the simulated and experimental results of quadruple junction silicon-based TFSCs. The best experimental cell exhibited a PCE of 15.03% [12]. Its $V_{oc}$ is 3.02 V, which is higher than our simulated result. This is because the structure of the experimental cell is a-$SiC_z$:H/a-Si:H/a-$Si_{1-x}Ge_x$:H/μc-Si:H, where the band gap of each sub-cells is correspondingly wider than that of the sub-cells in our cell model. Moreover, it can be found that the lower experimental cell efficiency is mainly caused by the decrease of the $J_{sc}$. One reason is that the μc-$Si_{0.5}Ge_{0.5}$:H bottom sub-cell can effectively extend the spectral response to 1300 nm, leading to a more efficient

utilization of the solar energy. The other reason is that the current matching of the quadruple junction TFSC is difficult in the experiment. Both the inappropriate bandgap and thickness of the sub-cells could cause the current loss. As we know, the matching of each sub-cells of quadruple junction TFSC can be quickly realized by theoretical calculation, which could effectively shorten the R&D circle time. Therefore, it is very necessary to introduce simulation technique into the development of quadruple junction TFSCs.

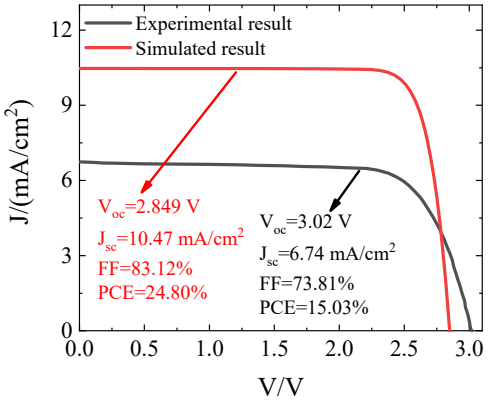


Fig. S1. Simulated and experimental results of quadruple junction silicon-based TFSCs.

## References


1. Liu Y, Sun Y, Liu W, Yao J. Novel high-efficiency crystalline-silicon-based compound heterojunction solar cells: HCT (heterojunction with compound thin-layer). Physical Chemistry Chemical Physics, 2014, 16(29): 15400-15410.
2. He J, Lu X, Li X, Dong Y, Yue F, Chen Y, Sun L, Yang P, Chu J. Compositional dependence of photovoltaic properties of $Cu_2ZnSnSe_4$ thin film solar cell: Experiment and simulation. Solar Energy, 2018, 159: 572-578.
3. Liu Y, Ahmadpour M, Adam J, Kjelstrup-Hansen J, Rubahn H G, Madsen M. Modeling multijunction solar cells by nonlocal tunneling and subcell analysis. IEEE Journal of Photovoltaics, 2018, 8(5): 1363-1369.
4. Cruz A, Wang E C, Morales-Vilches A B, Meza D, Neubert S, Szyszka B, Schlatmann R, Stannowski B. Effect of front TCO on the performance of rear-junction silicon heterojunction solar cells: Insights from simulations and experiments. Solar Energy Materials and Solar Cells, 2019, 195: 339-345.
5. Xue H, Birgersson E, Stangl R. Correlating variability of modeling parameters with

photovoltaic performance: Monte Carlo simulation of a meso-structured perovskite solar cell. Applied Energy, 2019, 237: 131-144.

6. Yu M, Li Y, Cheng Q, Li S. Numerical simulation of graphene/GaAs heterojunction solar cells. Solar Energy, 2019, 182: 453-461.
7. Pandey R, Saini A P, Chaujar R. Numerical simulations: Toward the design of 18.6% efficient and stable perovskite solar cell using reduced cerium oxide based ETL. Vacuum, 2019, 159: 173-181.
8. Azri F, Meftah A, Sengouga N, Meftah A. Electron and hole transport layers optimization by numerical simulation of a perovskite solar cell. Solar Energy, 2019, 181: 372-378.
9. Ferdaous M T, Shahahmadi S A, Chelvanathan P, Akhtaruzzaman M, Alharbi F H, Sopian K, Tiong S K, Amin N. Elucidating the role of interfacial $MoS_2$ layer in $Cu_2ZnSnS_4$ thin film solar cells by numerical analysis. Solar Energy, 2019, 178: 162-172.
10. Matsui T, Kondo M, Ogata K, Ozawa T, Isomura M. Influence of alloy composition on carrier transport and solar cell properties of hydrogenated microcrystalline silicon-germanium thin films. Applied Physics Letters, 2006, 89(14): 142115.
11. Huang Z H, Zhang J J, Ni J, Cao Y, Hu Z Y, Li C, Geng X H, Zhao Y. Numerical simulation of a triple-junction thin-film solar cell based on μc-Si1-xGex:H. Chinese Physics B, 2013, 22(9): 098803.
12. Liu B, Bai L, Li T, Wei C, Li B, Huang Q, Zhang D, Wang G, Zhao Y, Zhang X. High efficiency and high open-circuit voltage quadruple-junction silicon thin film solar cells for future electronic applications. Energy & Environmental Science, 2017, 10(5): 1134-1141.